

Direct Visualization of Defect Density Waves in 2D

L. Ottaviano,¹ A. V. Melechko,^{2,3} S. Santucci,¹ and E. W. Plummer^{2,3}

¹*INFN, Unità dell'Aquila, and Dipartimento di Fisica Università dell'Aquila, Via Vetoio 10, I-67010 Coppito L'Aquila, Italy*

²*Department of Physics and Astronomy, The University of Tennessee, Knoxville, Tennessee 37996*

³*Solid State Division, Oak Ridge National Laboratory, Oak Ridge, Tennessee 37831*

(Received 28 August 2000)

A scanning tunneling microscopy investigation of the $\frac{1}{3}$ of a monolayer α phase of Sn on Si(111) reveals a new low temperature phase, which is electronic and not structural. This phase consists of a one-dimensional incommensurate electronic wave that coincides with a periodic modulation of the population of the substitutional Si defects, i.e., a defect density wave.

DOI: 10.1103/PhysRevLett.86.1809

PACS numbers: 68.35.Rh, 68.35.Bs, 71.45.Lr, 72.10.Fk

It is generally recognized that the defects can play a critical role in phase transitions, especially in reduced dimensionality [1]. Mobile defects and the onset of their spatial long range ordering are often invoked as the microscopic explanation of some experimental observations in low temperature phase transitions, such as the occurrence of thermal hysteresis effects [2]. For example, it has been hypothesized that a modulation of the occupation probability of defects along the one-dimensional lattice occurs in potassium cyanoplatinide [2,3]. Even though the alignment of defects has not been directly demonstrated experimentally, the concept has proven to be a useful microscopic description for a variety of experimental data [2].

A variable temperature scanning tunneling microscope (STM) furnishes an ideal tool for the direct visualization of the role of defects in a two- or one-dimensional systems. Melechko *et al.* [4–6] have reported on the role of defects in the charge density wave (CDW) transition that occurs for ultrathin (α -phase) films of Pb and Sn on Ge(111). The α phase at room temperature (RT) is formed from one third of a monolayer of Sn or Pb, adsorbed on T_4 sites, on bulk terminated Ge(111) [7]. These films exhibit a CDW symmetry lowering transition from $\sqrt{3} \times \sqrt{3} \rightarrow 3 \times 3$ symmetry as the temperature is lowered [8,9]. In the Sn/Ge(111) system, there is a defect-mediated condensation of the CDW phase caused by an alignment of the Ge substitutional defects at ~ 120 K compatible with the three domains of the CDW phase [4,5]. Noteworthy is the observation that in the defect-free system Fermi surface nesting cannot drive this transition [9]. It has been proposed that defects are needed to allow for nesting [10].

This paper reports on a variable temperature STM investigation of the α phase of Sn on Si(111), down to a temperature of ~ 60 K. At RT, this system exhibits the same structure as the Sn/Ge system [11,12] with metallic character [13,14]. In contrast to the Sn/Ge(111) system, no (3×3) CDW has been reported as the temperature is lowered (~ 70 K) [15,16]. Our STM measurements reveal a new periodicity at low temperature not seen in electron diffraction, i.e., an electronic transition. In this low temperature phase of the Sn/Si(111) system,

the defects, primarily Si substitutional atoms, are aligned commensurate with the one-dimensional electronic wave (defect density wave), which appears to be incommensurate with the substrate. The α phase of Sn/Si(111) is fundamentally different than the isoelectronic Sn/Ge(111) system.

The experiments were performed using UHV omicron variable temperature STMs (30–300 K), equipped with standard surface preparation facilities and a LEED camera. The Si(111)-(7 \times 7) reconstructed substrates were prepared by direct resistive heating at 1250 °C for 1 min after outgassing for 12 h at dark glowing temperature (550 °C). The α phase of Sn/Si(111) ($\sqrt{3} \times \sqrt{3}$) was obtained by depositing $\frac{1}{3}$ of a monolayer of Sn at RT and then annealing it up to 650 °C in front of LEED until the $\sqrt{3} \times \sqrt{3}$ pattern was observed [15–17]. Our RT STM images were identical to those previously published [15–17].

Figure 1 summarizes our observations of the low temperature STM images at 60 ± 10 K. Figure 1(a) shows an empty state image and Fig. 1(c) shows a filled state image for a film with an average defect density of 4%. On the right are the Fourier transforms (FT) of the respective STM images. Never have we observed a (3×3) CDW phase with the STM. LEED observations are consistent with this statement [16]. A casual inspection of the empty state image in Fig. 1(a) reveals what looks similar to a new structure with the symmetry $(2\sqrt{3} \times \sqrt{3})R30^\circ$. The primitive lattice vectors for the $\sqrt{3} \times \sqrt{3}$ [$2\sqrt{3} \times \sqrt{3}$] structure are shown in the top-left [top-right] inset of Fig. 1(a). Defining the x axis as horizontal and y vertical in Fig. 1, the primitive lattice vectors of the $\sqrt{3} \times \sqrt{3}$ can be defined as $\mathbf{a}_1 = a\mathbf{i}$ and $\mathbf{a}_2 = a/2(-\mathbf{i} + \sqrt{3}\mathbf{j})$ with reciprocal lattice vectors given by $\mathbf{b}_1 = (2\pi/a)(\mathbf{i} + \mathbf{j}/\sqrt{3})$ and $\mathbf{b}_2 = (2\pi/a)(2/\sqrt{3})\mathbf{j}$. $a = 6.65 \text{ \AA}$ is the Sn-Sn nearest neighbor spacing. When the apparent $2\sqrt{3} \times \sqrt{3}$ structure forms, the new primitive lattice vectors are \mathbf{a}_1 and $2\mathbf{a}_2$, with reciprocal lattice vectors given by \mathbf{b}_1 and $\mathbf{b}_2/2$. The FTs of the empty and filled state images [Figs. 1(b) and 1(d)] clearly show the reciprocal lattice points indicative of the $(\sqrt{3} \times \sqrt{3})R30^\circ$ phase, and new reciprocal lattice points created by the new $2\sqrt{3}$ -like

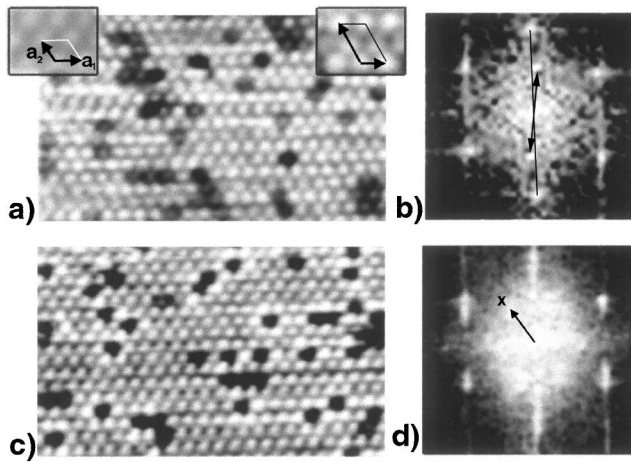


FIG. 1. STM images of the α phase of Sn/Si(111) at ~ 60 K: (a) Empty state (+1.5 V) STM image of an $153 \times 98 \text{ \AA}^2$ area showing $2\sqrt{3}$ -like structure. The $\sqrt{3} \times \sqrt{3}$ and $2\sqrt{3} \times \sqrt{3}$ unit cells are shown in the insets. (b) Fourier transform (FT) of an empty state image of $300 \text{ \AA} \times 300 \text{ \AA}$ containing the area imaged in (a). The $\sqrt{3} \times \sqrt{3}$ reciprocal lattice vectors are indicated (thin line) as well as (thick arrows) the spots corresponding to the 1D canted wave vector \mathbf{K}_c (see text). (c) Filled state (-1.5 V) STM image at ~ 60 K; (d) Fourier transform of the image of an area of $300 \times 300 \text{ \AA}^2$, containing the area shown in (c). An arrow indicates the \mathbf{k} -vector to the center of the diffused spot. X shows the correct position for (3×3) order.

periodicity seen in STM images. Again, there is no sign in the FTs of the (3×3) CDW phase.

The main conclusions based on the low temperature STM observations are the following.

(1) *There is no evidence for the (3×3) CDW phase seen for Sn and Pb on Ge(111).*—Even though we never see (3×3) diffraction or images [15], we see an increased background in LEED intensity in the area of (3×3) spots [18] similar to what was reported by Uhrberg *et al.* [16]. The real space image in Fig. 1(c) shows the origin of this periodicity. Around every defect is a bright nearest neighbor ring of Sn atoms, reminiscent of a RT image of Sn on Ge(111). This is the damped CDW induced by each defect. The difference between Sn on Ge and Sn on Si is that for Si the extent of the waves does not dramatically increase as the temperature is lowered [15]. The broad diffuse background in the region of the (3×3) of the FT of the filled state STM image [Fig. 1(d)] is due to the Sn nearest neighbor response to the Si defect. But the \mathbf{k} -vectors to the centers of these spots [shown by the arrow in Fig. 1(d)] are $\sim 15\%$ shorter than expected for (3×3) (marked by x). The wave induced by defects in Sn/Si(111) has a longer period than the waves in Sn/Ge(111). For comparison, similar diffuse spots in FT of RT STM images of Sn/Ge(111) are located exactly at the (3×3) positions [5]. The obvious conclusion of this observation is that the CDW (3×3) configuration is not the ground state of a defect-free or low defect α phase of Sn on Si(111) [19].

(2) *The one-dimensional structure is incommensurate and dependent upon the bias voltage.*—The bright spot in the FT of the filled state image [Fig. 1(d)] associated with the $2\sqrt{3}$ reconstruction is exactly where the new reciprocal lattice vector should be. In stark contrast, this spot in the empty state FT is not in the same position [see arrow and vertical line in Fig. 1(b)]. The spot is rotated slightly (7° – 8°) from the perpendicular $\langle 112 \rangle$ direction. This new vector can be described by the vector $\mathbf{K}_c = (2\pi/\sqrt{3}a)[(0.132 \pm 0.009)\mathbf{i} + \mathbf{j}]$. There is no reason to believe that this is a commensurate vector, but a new periodicity along the horizontal rows of seven or eight would fall in the experimental uncertainty. Once this new periodicity has been identified in the FT, it is easy to see it in the real space image [Fig. 1(a)]. Start with a bright atom and move along the horizontal rows; the bright rows seem to distort and become dim and then bright again. The “atoms” along a horizontal row in the empty state image are visibly laterally shifted from ideal T_4 position, i.e., rows are not straight. There is an electronic superstructure in the empty state image, which is 1D in character. It is clearly one dimensional because there are no additional diffraction spots that would be associated with a periodicity in the horizontal direction. For example, if this were a commensurate reconstruction of the form $2\sqrt{3} \times 7\sqrt{3}$, there would be many seventh order spots in the FT. It is electronic because it depends upon the bias voltage used to accumulate the STM image, and is not seen in the diffraction pattern.

It should be pointed out that, in practice, there are six different one-dimensional waves possible, two associated with each of the three $\sqrt{3}$ direction. In many large-scale images, where the lattice has been removed by filtering the FT, waves in multiple directions are observed. Occasionally, STM images contain a superposition of 1D waves in two directions leading to $2\sqrt{3} \times 2\sqrt{3}$ superstructure.

If a real space image is constructed to isolate the electronic distortion using only the “diffraction spots” in the FT, the defects will disappear unless they are ordered with this periodicity. This real space image has been fabricated in Fig. 2(a) by creating an image composed of the $\sqrt{3} \times \sqrt{3}$ spots and the canted spot (\mathbf{K}_c) seen in the empty state image of Fig. 1(b). In this artificial image, there are no imperfections and the electronic distortion of the horizontal rows of Sn is quite evident. Figure 2(b) is such a constructed real space image, where the $\sqrt{3} \times \sqrt{3}$ spots have been filtered out of the FT shown in Fig. 1(b) and then transformed back. This image reveals everything, if you look closely. There are bright and dark rows with the periodicity of the vector \mathbf{K}_c shown by the arrow in Fig. 1(b).

(3) *In the low temperature phase the defects have aligned into rows forming defect density waves.*—Most surprising is the fact that the defects seem to be aligned within the dark rows. To illustrate this alignment of defects or this defect density wave, a one-dimensional

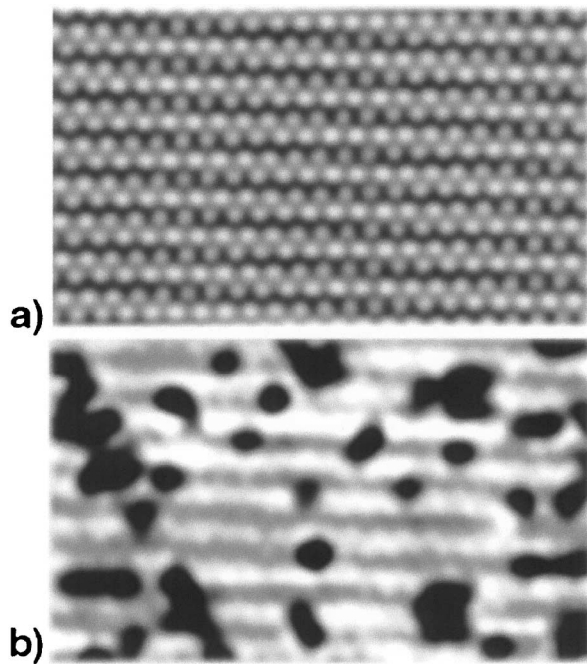


FIG. 2. (a) Real space empty state STM image simulated from the main spots of the FT of Fig. 1(b). (b) Back Fourier transform of Fig. 1(a) after filtering out the $\sqrt{3} \times \sqrt{3}$ spots of Fig. 1(b).

mask with a wavelength of $\lambda = 2\pi/\mathbf{K}_c$ has been placed on Fig. 1(a) and shown in Fig. 3. Here, one half of a wavelength is transparent and the other half opaque. With the alignment of the phase of the mask according to Fig. 2(b), the opaque sections cover the vast majority (75%) of the Si substitutional defects. The defects that are left not covered seem to be aligned in the other two directions rotated 120°. If the same procedure is used with the direction and wavelength of the mask given by the reciprocal lattice vector $\mathbf{K}_0 = \mathbf{b}_2/2$, associated with the $2\sqrt{3} \times \sqrt{3}$ structure, $\sim 50\%$ of the defects are exposed. Thus, we show that there is clearly periodic modulation of the defect density along the canted (\mathbf{K}_c) direction. This is the first direct experimental evidence of a one-dimensional



FIG. 3. Empty state STM image of Fig. 1(a) with a half transparent mask with a wavelength $\lambda = 2\pi/\mathbf{K}_c$. The dark segments of the mask cover 3/4 of all of the Si substitutional defects.

defect density wave (DDW). Measurements of the defects in a $\sqrt{3} \times \sqrt{3}$ phase at RT (never been cooled) show a random distribution. Defect alignment must be intimately associated with the formation of the new structure seen at low temperature with the STM.

(4) *The one-dimensional electron density wave and the aligned defect density wave do not create a measurable periodic lattice distortion.*—The apparent displacement of the atoms from the T_4 in the empty state image [Fig. 1(a)] is ~ 0.5 Å along the in-plane $2\sqrt{3}$ direction, and ~ 0.15 Å vertically. We have estimated the possible lattice distortion from the background intensity in LEED [20] compared to the LEED intensities observed for the Sn/Ge system. This leads to an estimate of a vertical distortion less than 0.02 Å and a horizontal distortion slightly larger. Therefore it is clear that the STM images are caused solely by a one-dimensional electronic wave.

In a detailed LEED-photoelectron spectroscopy study of this system as a function of Sn coverage and temperature, Uhrberg *et al.* reported that LEED shows no structural transition down to 70 K, but that there are dramatic changes in the electronic structure [16]. Combining the observations reported in this paper with what is reported by Uhrberg *et al.* leads to the conclusion that there is an electronic transition without an accompanying lattice distortion. The 1D electronic transition is accompanied by the 1D DDW.

Why is the behavior of the Sn/Si(111) system so different than the isoelectronic system Sn/Ge(111)? One possible explanation could be that the structure is different, but x-ray diffraction studies of these two systems [21] indicate almost no difference except for the inherent difference in the Si-Si and Ge-Ge bond length. The only obvious difference between these two systems is the band gap of the substrate. There are, in our opinion, two key experimental differences in these systems. First, it has been reported [22,23] and confirmed by this study that most of the Si atoms in substitutional sites in the Sn film are not in the T_4 sites as they are for the Sn/Ge system. Instead, they are displaced towards the H_3 sites, breaking the point group symmetry at the defect site. The local reduction in symmetry around a Si defect at RT [22] and the symmetry lowering long range ordering should be correlated. Second, the response of the two systems to the presence of defects is fundamentally different. For Sn on Ge there are temperature dependent damped CDW emanating from the defect indicating an instability in the system. In contrast, no such extended waves exist for the Sn/Si system [15]. It is interesting to note that the calculation of the Fermi surface and the response function performed for Sn/Ge(111) showed that Fermi surface nesting could occur near the vector associated with the formation of a $2\sqrt{3}$ CDW but not observed (3×3) CDW. The result presented in this paper could imply that Sn/Si(111) displays expected behavior, and that the Sn/Ge(111) system is abnormal.

In summary, we have shown with STM the occurrence of a one-dimensional defect density wave concurrent with a 1D electronic wave, which is apparently incommensurate with the underlying lattice. Together, the Sn/Ge and Sn/Si thin films systems present a magnificent arena for the study of the dynamics of defects in a two-dimensional phase transition. Undoubtedly, this is just the beginning, since there are far more questions than answers.

We thank H. H. Weitering and G. Profeta for fruitful discussions and R. I. Uhrberg and Ismail for help in estimating lattice distortion. The work of E. W. P. and A. V. M. was supported by the National Science Foundation Grant No. DMR 980130. Some of this work was conducted at Oak Ridge National Laboratory, managed by UT-Battelle, LLC, for the U.S. Department of Energy under Contract No. DE-AC05-00OR22725.

-
- [1] B. I. Halperin and C. M. Varma, *Phys. Rev. B* **14**, 4030 (1976).
- [2] I. Baldea and M. Badescu, *Phys. Rev. B* **48**, 8619 (1993).
- [3] I. Baldea and M. Apostol, *J. Phys. C* **18**, 6135 (1985).
- [4] A. V. Melechko, J. Braun, H. H. Weitering, and E. W. Plummer, *Phys. Rev. Lett.* **83**, 999 (1999).
- [5] A. V. Melechko, J. Braun, H. H. Weitering, and E. W. Plummer, *Phys. Rev. B* **61**, 2235 (2000).
- [6] H. H. Weitering, J. M. Carpinelli, A. V. Melechko, J. Zhang, M. Bartkowiak, and E. W. Plummer, *Science* **285**, 2107 (1999).
- [7] J. S. Pedersen, R. Feidenhans'l, M. Nielsen, and K. Kjaer, *Surf. Sci.* **189/190**, 1047 (1987).
- [8] J. M. Carpinelli, H. H. Weitering, M. Bartkowiak, E. W. Plummer, and R. Stumpf, *Nature (London)* **381**, 398 (1996).
- [9] J. M. Carpinelli, H. H. Weitering, M. Bartkowiak, R. Stumpf, and E. W. Plummer, *Phys. Rev. Lett.* **79**, 2859 (1997).
- [10] T. E. Kidd, T. Miller, M. Y. Chou, and T.-C. Chiang, *Phys. Rev. Lett.* **85**, 3684 (2000).
- [11] J. Nogami, S.-I. Park, and C. F. Quate, *J. Vac. Sci. Technol. A* **7**, 1919 (1989).
- [12] K. M. Conway, J. E. McDonald, and C. Norris, *Surf. Sci.* **215**, 555 (1989).
- [13] T. Kinoshita, S. Kono, and T. Sagawa, *Phys. Rev. B* **34**, 3011 (1986).
- [14] G. Profeta, A. Continenza, L. Ottaviano, and A. J. Freeman, *Phys. Rev. B* **62**, 1556 (2000).
- [15] L. Ottaviano, M. Crivellari, L. Lozzi, and S. Santucci, *Surf. Sci.* **445**, L41 (2000).
- [16] R. I. G. Uhrberg, H. M. Zhang, T. Balasubramanian, S. T. Jemander, N. Lin, and G. V. Hansson, *Phys. Rev. B* **62**, 8082 (2000).
- [17] C. Törnevik, M. Göthelid, M. Hammar, U. O. Karlsson, N. G. Nilsson, S. A. Flodström, C. Wigren, and M. Östling, *Surf. Sci.* **314**, 179 (1994).
- [18] A higher intensity background in the vicinity of (3×3) spots in the LEED pattern can be observed at high defect density.
- [19] F. Flores, J. Ortega, R. Pérez, A. Charrier, F. Thibaudau, J.-M. Debever, and J.-M. Themlin, *Prog. Surf. Sci.* (to be published).
- [20] R. I. Uhrberg (private communication).
- [21] O. Bunk, J. H. Zeysing, G. Falkenberg, R. L. Johnson, M. Nielsen, M. M. Nielsen, and R. Feidenhans'l, *Phys. Rev. Lett.* **83**, 2226 (1999).
- [22] L. Ottaviano, M. Crivellari, G. Profeta, A. Continenza, L. Lozzi, and S. Santucci, *J. Vac. Sci. Technol. A* **18**, 1946 (2000).
- [23] L. Ottaviano, G. Profeta, A. Continenza, S. Santucci, A. J. Freeman, and S. Modesti, *Surf. Sci.* **464**, 57 (2000).